Nr 7—8 (455—580) LIPIEC—SIERPIEŃ 2000 Tom XLV

P O L I M E R Y

MIESIĘCZNIK POŚWIĘCONY CHEMII, TECHNOLOGII I PRZETWÓRSTWU POLIMERÓW

R. F. T. STEPTO, J. I. CAIL, D. J. R. TAYLOR
Polymer Science and Technology Group
Manchester Materials Science Centre
UMIST and University of Manchester
Grosvenor St., Manchester
M1 7HS, UK

Polymer networks: principles of formation, structure and properties

Summary – This paper discusses the results of two types of theoretical investigations into the formation, structure and properties of polymer networks. First, to predict the value of the initial elastic modulus, it is important to be able to model, statistically, the molecular growth leading to network formation. A Monte-Carlo network polymerisation algorithm has been developed. It uses Flory-Stockmayer random-reaction statistics with intermolecular reaction allowed on a correctly weighted basis. The algorithm simulates, as a function of extent of reaction, the formation of all of the connections in a reaction mixture and counts all the ring structures. It also enables polymerisations and network structures to be simulated efficiently up to complete reaction. Comparisons of predictions from the algorithm with experimental data from end-linking polymerisations show the importance of accounting for the whole distribution of sizes of ring structure in determining reductions in elastic modulus. An important new factor, x, is introduced in the interpretation of experimental data. It is the fractional loss in elasticity per chain in loop structures larger than the smallest (eqns. 13—15, figs. 7, 8). The second type of investigation shows that Monte-Carlo simulations (fig. 10) of the elastic behaviour of chains in networks, using realistic (R-I-S) network-chain models, are able to reproduce experimentally observed deviations from Gaussian network behaviour in uniaxial extension (fig. 9). The finite extensibility of the network chains causes non-affine deformation of the mean-square network-chain end-to-end distance, even at moderate sample deformations ($\lambda \approx 1.5$). An increase in the proportion of fully extended chains with increasing macroscopic strain gives rise to a steady decrease in the rate of network free-energy change with strain, causing a reduction in the network modulus. There is no need to invoke a tran- sition from affine to phantom chain behaviour as deformation increases. For a complete understanding of the structure and elastomeric properties of polymer networks, both types of investigations need to be combined. Thus, the number and types of elastic-chains, including loop structures, and their entropy-deformation relationships would be known. The network

can then be deformed, and the values of initial modulus as well as stress-strain behaviour predicted.

Key words: network polymerisation, Monte-Carlo simulation, loop structures, elastomeric properties of polymer networks.

The molecular structures and macroscopic properties of network polymers depend more closely on reactant structures (molar masses, functionalities, chain flexibilities) and reaction conditions (dilution, proportions of different reactants) than do those of linear polymers. To understand and predict elastomeric properties, it is important to be able to model, statistically, the molecular growth leading to network formation. In Section 1, a new Monte-Carlo network polymerisation algorithm is used to simulate, as a function of extent of reaction, the formation of all of the connections in a reaction mixture and to count all the ring structures. It enables polymerisations and network structures to be simulated efficiently up to complete reaction.

In Section 2, Monte-Carlo simulations of the elastic behaviour of realistic network chains are described. The simulations are able to reproduce experimentally observed deviations from Gaussian network behaviour in uniaxial extension. The finite extensibility of the network chains is shown to cause non-affine deformation of the mean-square network-chain end-to-end distance, even at moderate sample deformations. There is no need to invoke a transition from affine to phantom chain behaviour as deformation increases.

NETWORK FORMATION, TOPOLOGY AND ELASTIC MODULUS (SECTION 1)

Perfect network formation

The classical Flory-Stockmayer (F-S) treatment of the gel point and the accompanying changes in distributions of molecular species give a basic explanation of the phenomena to which the behaviour and changes in actual polymerisations may be related. However, as discussed in detail by Flory [1], the infinite species, which occur from the gel point to complete reaction, cannot be enumerated as individual molecules. In addition, F-S theory says nothing concerning the detailed topology of the network, which grows and defines its structure through the random reaction of its reactive groups with other groups on the gel and with groups on sol species. To obtain a perfect network, all reactions (sol-sol, sol-gel and gel-gel) are assumed to yield elastically active chains between junction points in the final network. This assumption is rarely true and will be examined in detail in this part of the paper.

The elastomeric properties of polymer networks depend to a large extent on the value of the molar mass of the elastically active chain connecting a pair of junction points, M_c. If a perfect network structure is assumed then M_c can be calculated directly from the reactant structures, taking account of unreacted groups for non-stoichiometric reaction mixtures. In general, the detailed relationship between M_c and reactant structures depends on reactant architectures as well as extents of reaction and it is not possible to give a completely general formula [2—4]. However, formula for M_c from most stoichiometric end-linking polymerisations (using star reactants) at complete reaction can be derived relatively simply by assuming the perfect network structure and relating it to the structures of the reactants from which it is formed. For RA_2 + $R'B_f$ polymerisations, if N_c is the number of chains between junction points and N_j the number of junction points,

$$\frac{N_c}{N_j} = \frac{f}{2} \tag{1}$$

as $f/2$ chains emanate from each junction. Also, M_c is simply the molar mass of two arms of the $R'B_f$ unit plus the molar mass of the RA_2 unit.

Relationships between concentrations of chains and junction points that assume perfect network structures are often used when interpreting elastic properties of end-linked networks [5]. All chains and junction points are assumed to be elastically active and one may replace the symbols N_c and N_j by N_{ec} and N_{ej}, denoting the numbers of elastically active chains and junction points. In practice, deviations from these assumptions occur and the values of N_{ec} or N_{ej} deduced from elastomeric properties are rarely those expected from the amount of chemical reaction that has occurred. Such deviations may be due to topological entanglements and chain interactions [6—10], to side reactions, incomplete reaction in end-linking polymerisations (giving loose ends) [11, 12] and, more fundamentally and generally, inelastic chain or loop formation due to the intermolecular reaction of pairs of groups [2—4, 10].

It is obviously important for predicting and interpreting the elastomeric properties of networks to be able to calculate the value of N_{ec} , N_{ej} or M_c from the reactants and the reaction conditions used. For stoichiometric RA_2 + $R'B_f$ polymerisations at complete reaction, one may write

$$M_c^o = \frac{W_{net}}{N_{ec}^o} \tag{2}$$

where W_{net} — *the mass of the network,* M_c^o *and* N_{ec}^o *refer to the perfect network structure.*

In reality, due to intermolecular reaction the actual number of elastic chains, N_{ec}, is less than N_{ec}^o, giving

$$M_c = \frac{W_{net}}{N_{ec}} \tag{3}$$

with $M_c > M_c^o$. Thus, M_c may be considered as a key quantity to consider, both experimentally and theoretically.

Elastic modulus

The close connection between network structures and modulus (G) is summarised by the equations, based on the application of Gaussian elasticity theory to uniaxial deformation [2—5],

$$\sigma = G(\Lambda - \Lambda^{-2}) \tag{4}$$

and

$$G = ART\rho\phi_2^{1/3}(V_u / V_F)^{2/3} / M_c \tag{5}$$

Equations (4) and (5) are valid at relatively low deformations. G is the shear modulus measured at zero frequency, σ is the applied stress per undeformed area and Λ the experimental deformation ratio. In the absence of free chain-ends, A has the values of $(1 - 2/f)$ and 1 for phantom and affine chain behaviours, respectively. Also, A may be put equal to 1 for values of Λ near 1. ρ is the density of the dry network, ϕ_2 the volume fraction of network during measurement (ϕ_2=1 for unswollen networks having no sol fraction), V_u is the volume of the dry, unstrained network and V_F the volume at formation (assumed to be equivalent to V_o, the volume in the strain-free reference state.) Hence, values of M_c may be deduced from measurements of modulus using equation (5). For dry networks, prepared in bulk $V_u = V_F$, $\phi_2 = 1$ and, for measurements at small deformations,

$$G = \frac{\rho}{M_c} \cdot RT = \frac{N_{cc}}{V_{cc}} \cdot RT = n_{cc}RT \tag{6}$$

where n_{cc} — *the molar concentration of elastic chains.*

Intramolecular reaction

In network-forming polymerisations, the increasing numbers of reactive groups per molecule, together with the spatial correlations between groups on the same molecule, mean that intramolecular reaction cannot generally be neglected. For -A + B- polymerisations, intramolecular reaction can be characterised in terms of the parameter P_{ab} for the smallest loop [2—4, 13, 14]

$$P_{ab} = \frac{P(r = 0)}{N_{Av}} \tag{7}$$

where $P(r = 0)$ — *the probability density of a zero end-to-end vector between reactive groups.*

P_{ab} thus represents the mutual concentration of A- and B-groups at the ends of the shortest sub-chain that can react intramolecularly. The structure of this sub-chain, consisting of v skeletal bonds, and of root-mean-square end-to-end distance $<r^2>^{1/2}$, is shown in figure 1. If it is assumed that the end-to-end distance

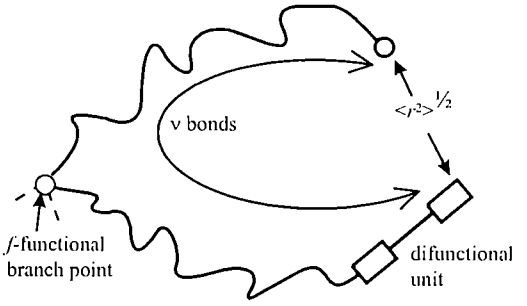

Fig. 1. Sub-chain forming a smallest loop structure illustrated with respect to an RA_2+RB'_f polymerisation. The diagram shows two arms of a star reactant, one arm having reacted with a difunctional monomer. The root-mean-square distance of the chain of n bonds between the terminal groups is $<r^2>^{1/2}$

distribution can be represented by a Gaussian function, P_{ab} is given by

$$P_{ab} = \frac{1}{N_{Av}}\left\{\frac{3}{2\pi < r^2 >}\right\}^{3/2} \tag{8}$$

Since the units of P_{ab} are moles per unit volume, it can be described as the mutual concentration of a pair of reactive groups on the same molecule that can react intramolecularly [2—4]. Accordingly, a useful measure of the propensity of a system at a given ratio of reactants for intermolecular reaction is λ_{a0}, where

$$\lambda_{a0} = \frac{P_{ab}}{c_{a0}} \tag{9}$$

with c_{a0}, *the initial concentration of A-groups, representing the concentration of groups for intermolecular reaction [2—4].*

λ_{a0} captures the combined effects of reactant structures and reactive-group concentrations on intramolecular reaction. A decrease in chain length or chain stiffness (*i.e.*, a decrease in $<r^2>$) results in an increase in P_{ab} and, hence, in the probability of intramolecular reaction and the formation of loop structures. Similarly, decreasing the concentration of reactive groups (c_{a0}) enhances the probability of intramolecular reaction.

Experimental results for polyurethane (PU) networks

The results to be discussed in detail in the present paper come from six series of PU-network materials formed via stoichiometric RA_2+$R'B_f$ polymerisations, using hexamethylene diisocyanate (HDI) and star polyoxypropylene (POP) polyols at different initial dilutions in nitrobenzene [15, 16]. The structure of the polyol ($R'B_f$) was varied in order to examine the effects of branch-point functionality (f) and reactant sub-chain length (v) on the moduli of the resulting networks. The six reaction systems are listed in table 1. As described in equation 2,

T a b l e 1: Functionalities, f, numbers of skeletal bonds, v, in the sub-chains forming the smallest possible loops, and elastic chain molar masses in the perfect networks, M_c^o, for six series of stoichiometric PU-forming, nonlinear polymerisations [15, 16]. The calculated values, using detailed conformational analyses [17], of the mean-square end-to-end distances, $\langle r^2 \rangle$, of the sub-chains of v bonds embedded in branched structures are also given.

PU system	f	v	M_c^o g · mol^{-1}	$\langle r^2 \rangle$, nm^2
1. HDI + POP triol	3	35	635	3.718
2. HDI + POP triol	3	62	1168	6.877
3. HDI + POP tetrol	4	28	500	2.753
4. HDI + POP tetrol	4	32	586	3.628
5. HDI + POP tetrol	4	43	789	4.605
6. HDI + POP tetrol	4	65	1220	6.581

M_c^o is the network-chain molar mass in the perfect network and is defined by the reactant structures. By rearranging the sections of the sub-chain illustrated in figure 1, it is easy to show that M_c^o is also the molar mass of the sub-chain of v skeletal bonds [16]. The values of $\langle r^2 \rangle$ listed in table 1 enable values of P_{ab} to be calculated using equation (8).

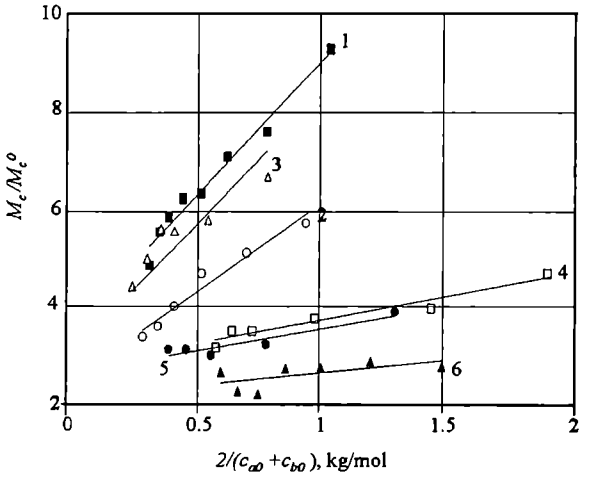

Fig. 2. Experimental values of M_c/M_c^o at complete reaction as functions of the average initial dilution of reactive groups, $2/(c_{a0}+c_{b0})$, for the six series of PU networks of table 1

Figure 2 shows plots of the values of M_c, relative to M_c^o for the perfect networks (M_c/M_c^o), as functions of the average initial dilution of reactive groups, $2/(c_{a0}+c_{b0})$, for the six series of PU networks formed at complete reaction. The values of M_c were determined from uniaxial compression measurements on dry and swollen networks and analysis of the results using equations (4) and (5). For each of the six experimental systems, an increase in the initial dilution of reactive groups results in a larger reduction in modulus, consistent with an increased incidence of intramolecular reaction and the formation of inelastic loop structures. The positive slopes of the plots indicate that direct relationships exist between intramolecular reaction (which increases with reactant dilution) and the network defects at complete reaction. This in itself shows that the dominant network defects are inelastic loop structures that can form both pre-gel and post-gel.

The plots in figure 2 show clearly that the magnitudes of the experimentally observed reductions in modulus are by no means insignificant. If perfect networks are formed, then $M_c/M_c^o = 1$. Hence, there is almost a ten-fold decrease in modulus in the case of the dry (bulk) network formed from the short-chain triol (system 1; $M_c^o = 635$ g mol^{-1}) at the highest initial dilution of reactive groups. For a given branch-point functionality, an increase in sub-chain length (v) results in a decrease in M_c/M_c^o, due to the decrease in the probability of loop formation (since $\langle r^2 \rangle$ in equation (8) increases). At approximately the same values of v, the reductions in moduli for tetrafunctional networks are considerably less than those of trifunctional ones. To a first approximation, this can be understood [10], on the basis of the different effects of the smallest loops that can form during $f = 3$ and $f = 4$ polymerisations.

Also, it should be noted that if the perfect networks were to exhibit phantom rather than affine behaviour, then $A = (1 - 2/f)$ (equation (5)) and for $f = 3$, $M_c/AM_c^o = 3$, and for $f = 4$, $M_c/AM_c^o = 2$. The observed values of M_c/M_c^o (or M_c/AM_c^o) are greater, therefore, than those for perfect networks assuming either affine or phantom behaviour.

General effects of loops on elasticity

The effects of the smallest and next smallest loop structures on the loss of network elasticity are illustrated in figure 3 for trifunctional and tetrafunctional networks. In perfect f-functional networks, each junction provides $f/2$ elastic chains. In the case of $f = 3$, each smallest loop structure renders two branch points inela-

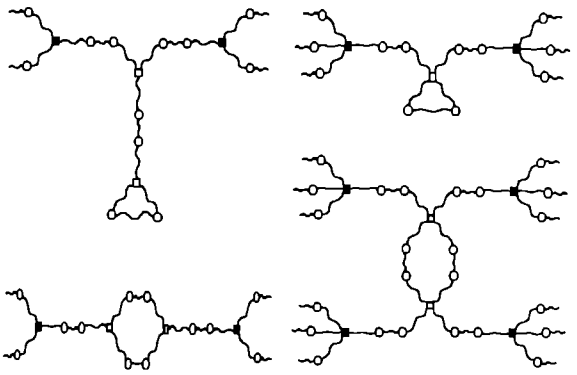

Fig. 3. Smallest (one-membered) and next smallest (two-membered) loop structures in trifunctional and tetrafunctional networks. ○ represents a reacted pair of groups; ■ denotes a fully-elastic junction point; ▩ denotes a junction point of reduced elasticity; □ denotes an elastically-inactive junction point

stic (shown as □ in the diagram), which is equivalent to the loss of three elastic chains. For $f = 4$, the effect is reduced; each loop is associated with the loss of a single elastic branch point, or two elastic chains. As a result, trifunctional networks are expected to be the more sensitive to loop defects, and decreases in modulus are expected to be greater than those of tetrafunctional networks with similar values of M_c^o, consistent with the experimental data in figure 2.

Unlike the smallest loops, larger loop structures do not disrupt the continuity of the network structure, and therefore network chains in larger loops are capable of supporting a load. The two-membered loop structures for trifunctional and tetrafunctional networks are also shown in figure 2. The question as to how larger loop structures contribute to losses in network elasticity remains unanswered. The conformational entropy of a large loop structure will be reduced [3, 18, 19], relative to that of an unperturbed, free linear chain of the same number of skeletal bonds, due to the decrease in the total number of possible chain conformations resulting from the constraints imposed by branch points along the chain and at the two chain ends. Since the origin of rubber-like elasticity lies in the conformational entropy of the network chains, any decrease in entropy should manifest itself as a decrease in the elasticity of the real network structure relative to that of the hypothetical, perfect one, whose network chains are assumed to be indistinguishable from the corresponding set of unperturbed (free) chains.

Monte-Carlo polymerisation algorithm

Theories to predict the modulus of a network material must begin by constructing a realistic model of the network structure, including defects [18, 20—22]. Detailed characterisation of the connectivity, or topology, by conventional, experimental means is impossible. In order to investigate the effects of network topology on elastomeric properties one must therefore use numerical simulations of the network-forming non-linear polymerisations. These have the potential to provide the necessary detailed structural information. In such simulations, it is important to account correctly for the formation of loop structures of various sizes resulting from intramolecular reactions, correctly weighted according to their probabilities of formation. To these ends, a Monte-Carlo (M-C) non-linear polymerisation algorithm, originally devised by Dutton, Stepto and Taylor [18] has been further developed [4] to simulate self-polymerisations (RA_f), and two-monomer polymerisations of the general type RA_2+$R'B_f$. During the course of a simulated polymerisation, populations of monomer units are connected together according to the relative probabilities for intramolecular and intermolecular reactions, using λ_{a0} and taking account of possible loop sizes and the decreasing external concentration of reactive groups as a polymerisation proceeds. All the connections are recorded as a function of extent of reaction of A- or B-groups, along with the calculated sol and gel fractions, and average degrees of polymerisation.

Loop-size distributions and extents of intermolecular reaction

The general description and operation of the algorithm have been described elsewhere [22]. Here, we concentrate on findings relevant to the experimental results in figure 2. Accordingly, figure 4 shows distributions at

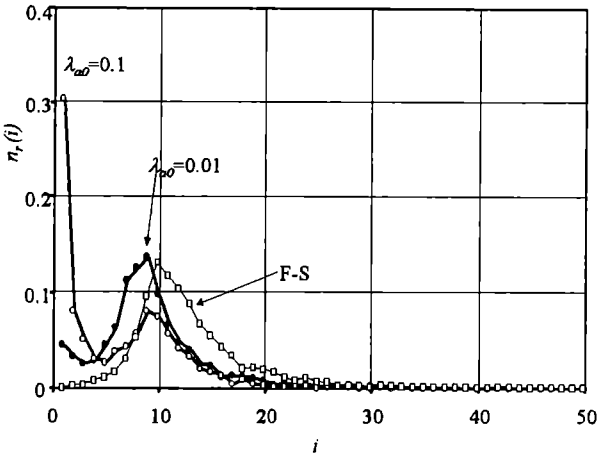

Fig. 4. RA_2+$R'B_4$ simulations at complete reaction. Overall number-fraction loop-size distributions for F-S, λ_{a0} = 0.01 and λ_{a0} = 0.01 simulations, each containing 1000 branch units

complete reaction for an F-S polymerisation and polymerisations with λ_{a0} = 0.01 and 0.1. The number fraction of loop structures of i repeat units, $n_r(i)$, is plotted against i.

$$n_r(i) = \frac{N_r(i)}{\sum_i N_r(i)} \tag{10}$$

where $N_r(i)$ *denotes the number of loop structures of size* i.

The F-S simulation was achieved by modifying the algorithm to exclude sol-sol and sol-gel intermolecular reaction and to allow only random intermolecular reaction on the largest species beyond the F-S gel point, *i.e.*, random gel-gel reaction. The fraction of smallest loops is negligible under F-S conditions. However, it is clearly seen that smallest loops start to dominate as λ_{a0} increases. Maxima in the distributions arise because of the changing different numbers of opportunities for forming loop structures of various sizes, integrated over all post-gel reaction. Also, the maximum is shifted to slightly smaller loop sizes in the simulations using λ_{a0} compared with those using F-S statistics. This is to be expected since intermolecular reaction is then biased towards the formation of smaller loops.

The changes in the calculated loop-size distributions

in the gel molecule at complete reaction with increasing λ_{a0} can be simply characterised by calculating extents of intermolecular reaction on that molecule resulting in smallest loops by the end (*e*) of a polymerisation, $p_{re,\,1}$, as a function of λ_{a0}. Such a characterisation is useful because the exact effects of smallest loops on network elasticity can be deduced (see Figure 3). In addition, $p_{re,\,i>1}$, the extent of reaction resulting in the formation of larger loops may also be calculated, so that the total, final extent of intermolecular reaction may be written

$$p_{re,\,total} = p_{re,\,i} + p_{re,\,i>1} \tag{11}$$

For illustration, the values of $p_{re,\,total}$, $p_{re,\,i}$ and $p_{re,\,i>1}$ for a series of RA_2+R'B_3 simulations are shown in figure 5. Notice that $p_{re,\,total} = 1/6$, always. This is related to the cycle rank of the completed network. For a stoichiometric RA_2+R'B_f polymerisation at complete reaction [23], $p_{re,\,total} = (1/2)(1 - 2/f)$.

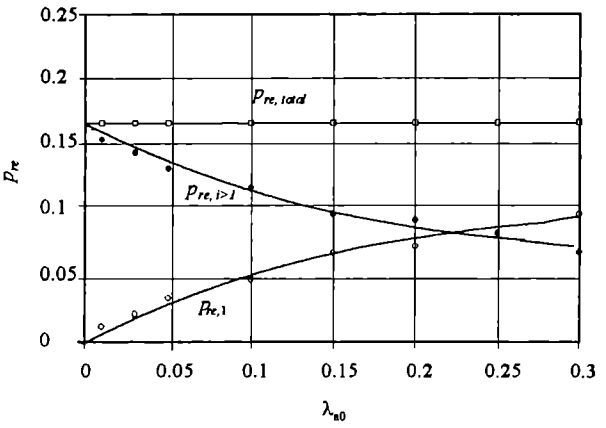

Fig. 5. $p_{re,\,total}$, $p_{re,\,1}$ and $p_{re,\,i>1}$ versus λ_{a0} for RA_2+R'B_3 simulations with 1000 branch units

Figure 5 shows that the incidence of smallest loops ($p_{re,\,1}$) is negligible when $\lambda_{a0} = 0$. Essentially, in agreement with F-S statistics and the results in figure 4, all intermolecular reaction then occurs after the gel point, resulting in larger loop structures. However, as λ_{a0} increases, $p_{re,\,1}$ increases at the expense of the proportion of larger loop structures ($p_{re,\,i>1}$). For a given value of λ_{a0}, it is found that tetrafunctional systems give rise to more loop structures than trifunctional systems, simply due to the greater number of opportunities for loop-formation in the former case. However, relative to the total number of loop structures, the proportion of smallest loops appears to be fairly insensitive to the branch-point functionality [22].

Correlation of model network topologies with measured network moduli

If the number of chains rendered elastically ineffective because of loop structures, N_e^l, can be estimated, the reduction in modulus, or increase in M_e, can be calculated using

$$\frac{M_e}{M_e^o} = \frac{N_{ee}^o}{N_{ee}} = \frac{N_{ee}^o}{N_{ee}^o - N_e^l} \tag{12}$$

From equation 1, $N_{ee}^o = N_f \cdot f/2$ and the quantity N_e^l may be estimated, approximately, using $p_{re,\,i}$ and $p_{re,\,i>1}$ from the M-C simulations.

For a trifunctional network of N_f branch units, the number of smallest loops is given by $3N_f\,p_{re,\,1}$, which means a loss of elastic chains equal to $3 \times 3N_f\,p_{re,\,1}$. However, the $3 \times 3N_f\,p_{re,\,i>1}$ chains in larger loops are subject only to a partial loss in elasticity, and may be taken as equivalent to $x \times 3 \times 3N_f\,p_{re,\,i>1}$ chains, where x is the fractional loss in elasticity per chain in a larger loop structure ($x = 1$ corresponds to a total loss in elasticity, seen in the case of smallest loops only). Hence, for $f = 3$

$$N_e^l = \frac{3N_f}{2} \cdot (6p_{re,1} + x \cdot 6p_{re,i>1}), \tag{13}$$

and substituting for N_e^l and N_{ee}^o in equation (12) yields

$$\frac{M_e}{M_e^o} = \frac{1}{1 - 6p_{re,1} - x \cdot 6p_{re,i>1}}. \tag{14}$$

A similar expression can be derived for tetrafunctional network structures. They lose only 2 elastic chains per smallest loop and

$$\frac{M_e}{M_e^o} = \frac{1}{1 - 4p_{re,1} - x \cdot 4p_{re,i>1}} \tag{15}$$

Estimates of x, the fractional loss of elasticity for chains in larger loop structures, can be made using the experimentally determined values of M_e/M_e^o for the series of PU networks in figure 2, in conjunction with simulated values of $p_{re,\,1}$ and $p_{re,\,i>1}$ and equations (14) and (15). However, since $p_{re,\,1}$ and $p_{re,\,i>1}$ calculated via the M-C simulations are dependent upon P_{ab}, values of M_e/M_e^o depend on both x *and* P_{ab}. Correlations between M-C calculations and experimental data may therefore be performed in two ways:

i) bivariate least-squares fitting, to evaluate both x and P_{ab}

ii) monovariate least-squares fitting, to evaluate x using P_{ab} values calculated *ab initio*, via chain-conformational analyses [17] leading to the values of $\langle r^2 \rangle$ in table 1.

The calculated values of x and P_{ab} for PU systems 1 to 6 are listed in table 2 and the fittings of the experimen-

Table 2: Values of x and P_{ab} based on correlations of experimentally-measured reductions in moduli for PU networks, and extents of intramolecular reaction calculated from M-C simulations. [a]bivariate fitting; [b]monovariate fitting with P_{ab} values calculated *ab initio*, using $\langle r^2 \rangle$ values from table 1.

PU system	f	x^a	P_{ab}^a, mol·L^{-1}	x^b	P_{ab}^b, mol·L^{-1}
1	3	0.667	0.538	0.816	0.076
2	3	0.599	0.103	0.690	0.030
3	4	0.684	0.547	0.775	0.120
4	4	0.638	0.457	0.730	0.079
5	4	0.582	0.129	0.637	0.055
6	4	0.481	0.088	0.559	0.032

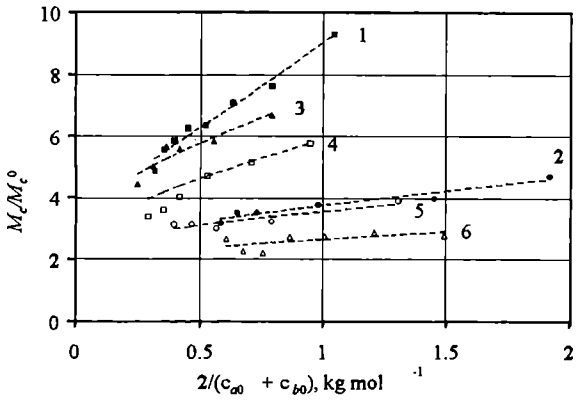

Fig. 6. M_c/M_c^o versus average initial dilution of reactive groups, $2/(c_{a0}+c_{b0})$, for the PU systems of table 1 and figure 3. Experimental values of M_c/M_c^o and calculated values using the bivariate analysis

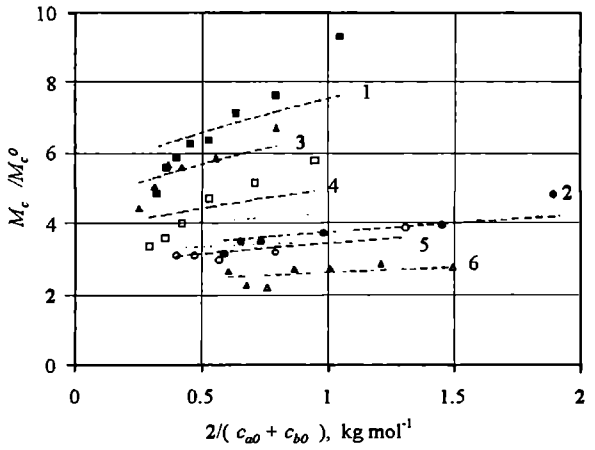

Fig. 7. M_c/M_c^o versus average initial dilution of reactive groups, $2/(c_{a0}+c_{b0})$, for the PU systems of table 1 and figure 3. Experimental values of M_c/M_c^o and calculated values using the monovariate analysis

tal M_c/M_c^o data using the bivariate and monovariate analyses are shown, respectively, in figures 6 and 7. The bivariate analysis results in very good fits to the experimental data and values of x in the range 0.67 to 0.60 are required to reproduce the experimental modulus reductions for the trifunctional PU networks (systems 1 and 2), and 0.68 to 0.48 for the tetrafunctional PU networks (systems 3 to 6). In both cases, an increase in the size of the smallest loop structure results in a decrease in x, indicating less elasticity lost. The values of P_{ab} estimated from the bivariate fitting are much higher than those calculated via $\langle r^2 \rangle$ for the sub-chain structures. Also, use of the *ab initio* calculated values of P_{ab} in the monovariate analysis results in a worse fitting of the experimental data at the higher values of M_c/M_c^o, but acceptable values of x are still required (x = 0.82 - 0.69, for f = 3, and 0.78 - 0.56 for f = 4).

Finally, figure 8 illustrates the effects of assuming that x = 0 (*i.e.* no additional loss in elasticity from larger

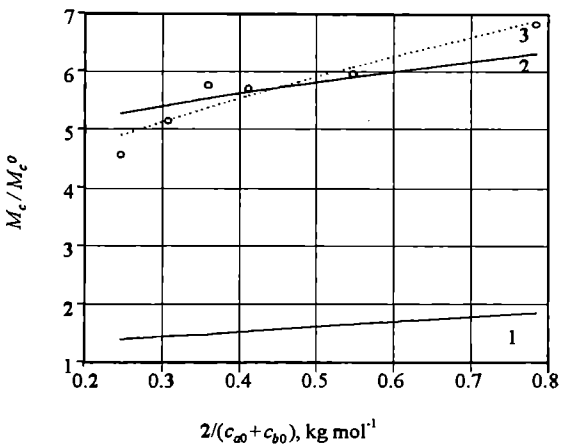

Fig. 8. M_c/M_c^o versus average initial dilution of reactive groups, $2/(c_{a0}+c_{b0})$, for PU system 3 of table 1 and figure 3. Experimental values of M_c/M_c^o and calculated values using the bivariate and monovariate analyses and the equation (15) with x = 0 and the ab initio value of P_{ab}; 1) x = 0, P_{ab} = 0.120 (from conformational calc.); 2) x = 0.775, P_{ab} = 0.120 (from conformational calc.); 3) x = 0.684, P_{ab} = 0.547

loop structures). The experimental data from system 3 are shown in comparison with the results from the bivariate and monovariate analyses and the monovariate analysis with x = 0. It is obvious that the neglect of the loss of elasticity in larger loop structures results in a gross underestimation of the experimentally observed reductions in moduli. The effects of the values used for P_{ab} are secondary compared with the effects of assuming x = 0.

THE ELASTIC BEHAVIOUR OF REAL CHAINS IN POLYMER NETWORKS (SECTION 2)

In this section, it is assumed that the concentration of elastic chains in a network is known and that all elastic chains are identical. These are the assumptions commonly used when treating the elastic behaviour of polymer networks. Upon moderate macroscopic deformation the elastic restoring force can be attributed to the deformation, and associated reduction in entropy, of the individual molecular chains connecting the network junction points [24—26]. Although the molecular origin of the elastic force in a rubber-like material has long been acknowledged, the relationships between deformations at macroscopic and molecular levels are not yet fully understood. It is thought that the initial network-chain deformation accompanying sample deformations is affine in the macroscopic strain, giving rise to the experimentally observed initial network modulus; as macroscopic deformation increases, the modulus is seen to decrease as the network chain deformation becomes less affine [25—27]. Finally, as more and more chains reach full extension, the network modulus increases rapidly (before sample rupture), due to the onset

of stress-induced crystallisation, or as a result of energy changes associated with valence-angle deformation and bond stretching.

The present theoretical approach elucidates the molecular origins of the observed decrease in the modulus of polymer networks at moderate sample deformations, taking networks of poly(dimethylsiloxane) (PDMS) chains as examples. Using a series of Monte-Carlo (M-C) calculations, the elastic properties of PDMS networks are related to the network-chain end-to-end distance distribution, and are therefore assumed to arise solely as a result of conformational changes in the network chains.

Numerical calculations

The first stage in the M-C simulation involves the numerical generation of the radial end-to-end distance distribution, $W(r)$, for unperturbed chains of various numbers of skeletal bonds (n) at a fixed temperature according to a rotational-isometric-state (R-I-S) or other realistic model. The corresponding values of probability density $P(r)$, are evaluated as $W(r)/4\pi r^2$, assuming the random orientation of chains in three dimensions. For PDMS, the Flory-Crescenzi-Mark R-I-S model [28] was used [29, 30].

The second stage of the numerical work concerns simulation of the elastic behaviour of a network. The "network" is represented by a spherically symmetrical sample of individual chains of a given number of bonds in a Cartesian laboratory-reference frame; one end of each chain is fixed at the origin. The chains are deformed uniaxially by a deformation ratio, λ, with $\lambda_x\lambda_y\lambda_z = 1$ (*i.e.* constancy of volume). The end-to-end distances are allowed to increase only up to their effective, conformational maximum, r^*_{max}, above which $W(r) = 0$. For an individual polymer chain, in a network of N chains, the Helmholtz free-energy change upon deformation at an absolute temperature T, is assumed to arise solely from the corresponding entropic change. Hence

$$\Delta A / NkT = \ln\{P(r_0) / r_{def})\} \tag{16}$$

where *the subscripts "0" and "def" denote the relaxed and deformed end-to-end vectors, respectively.*

In the M-C scheme, a chain with end-to-end distance r_0, is first chosen, in proportion to $W(r_0)$. The X- and Y-coordinates of its "free" chain-end are chosen randomly, and the Z-component defined consistent with r_0. Uniaxial deformations, using a series of values of λ are applied in the Z-direction (*i.e.* $\lambda = \lambda_z$) and the deformed end-to-end distances calculated by simple geometry, with $\lambda_x = \lambda_y = 1/\sqrt{\lambda}$. Any values of r_{def} in excess of r^*_{max} are put equal to r^*_{max}, thus limiting r to the range of values determined by the bond-conformational energies and consistent with $W(r)$. The associated value of $W(r_{def})$ is ascertained, and hence ln $P(r_{def})$ evaluated as before. The Helmholtz free-energy change is evaluated via equation 16, and the average change per chain at each λ calculated as

$$\Delta A / NkT = \frac{1}{N}\sum_{i=1}^{N} \ln\{P(r_0) / P(r_{def})\} \tag{17}$$

where N *is the number of chains in the M-C sample. Typically,* $N = 5 \times 10^6$.

Network simulation — analysis of results

Chain behaviour in uniaxial extension and compression may be compared by defining λ^* (< 1), the conjugate uniaxial compression ratio which produces the same value of $< r^2_{def} >$ *as* λ, the uniaxial extension ratio. For affine chain deformation at constant volume

$$< r^2_{def} > = (< r_0^2 > /3)(\lambda_x^2 + \lambda_y^2 + \lambda_z^2) = (< r_0^2 > /3)(\lambda^2 + 2/\lambda) \tag{18}$$

If $\lambda > 1$, then

$$\lambda^* = \lambda / 2\{(1 + 8/\lambda^3)^{1/2} - 1\} \tag{19}$$

will produce the same value of $< r^2_{def} >$.

The network Helmholtz free-energy change can be expressed as

$$\Delta A / NkT = s(\lambda^2 + 2/\lambda - 3) \tag{20}$$

for so-called Gaussian networks, with affine chain deformation [24, 25], a plot of $\Delta A/NkT$ versus $\lambda^2 + 2/\lambda - 3$ is linear, with $s = 1/2$. In general, s will be a function of λ and the corresponding normalised stress per unit unstrained cross-sectional area is

$$\frac{\sigma}{RT\rho} = \frac{1}{M_c}\left\{2s(\lambda - 1/\lambda^2) + (\lambda^2 + 2/\lambda - 3)\frac{\partial s}{\partial \lambda}\right\} \tag{21}$$

The values of s and $(\lambda^2 + 2/\lambda - 3)\partial s/\partial \lambda$ effectively describe the deviation of the simulated elastic behaviour from that of a bulk Gaussian network (with the same M_c), for which $s = 1/2$, $\partial s/\partial\lambda = 0$ and $\sigma = (\rho RT/M_c)(\lambda - 1/\lambda^2)$.

Theoretical results and discussion

The dependence of $\Delta A/NkT$ on $\lambda^2 + 2/\lambda - 3$ is shown in Fig. 9 for networks of PDMS chains of various lengths. The earlier departure from affine, Gaussian behaviour in uniaxial extension compared with compression is apparent. The results also show that $s \rightarrow 1/2$ with increasing network chain length, as expected.

The normalised stress, $\sigma/RT\rho$, may be calculated using equation 21, in conjunction with the values of s and $\partial s/\partial\lambda$, evaluated from the first and second derivatives of the plots in figures 9a & 9b. It may then be converted to normalised reduced stress, $[\sigma^*]/RT\rho$, where

$$[\sigma^*] = \frac{\sigma}{\lambda - 1/\lambda^2} \tag{22}$$

Conventionally, the effects of non-Gaussian, non-affine behaviour are represented as positive slopes of the so-called Mooney-Rivlin plots, $[\sigma^*]$ versus $1/\lambda$ (see [26]).

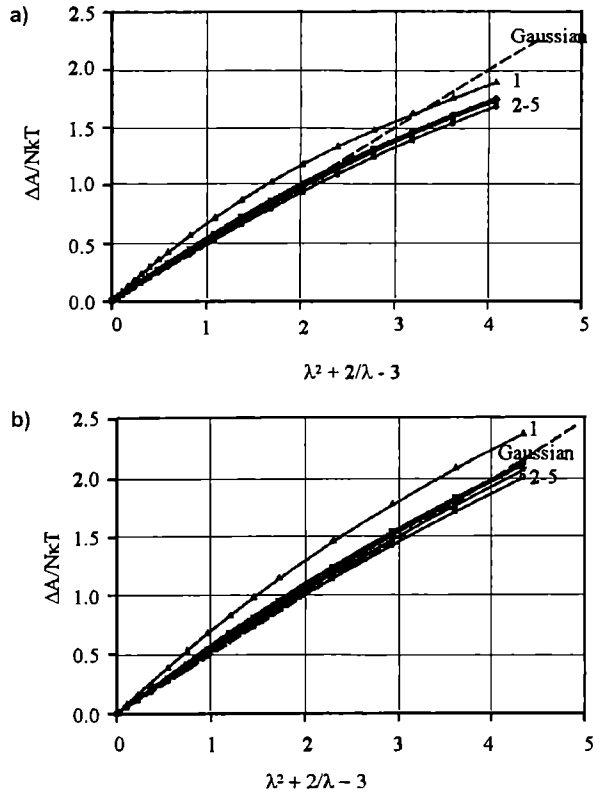

Fig. 9. Helmholtz energy change in uniaxial network extension as a function of $\lambda^2 + 2/\lambda - 3$ for PDMS chains of various numbers of skeletal bonds (n) at 298K; number of bonds: 1 — 40; 2 — 60; 3 — 80; 4 — 100; 5 — 150; a) extension, $\lambda = 1$ to 2.5; b) compresion, $\lambda = 1$ to 0.16

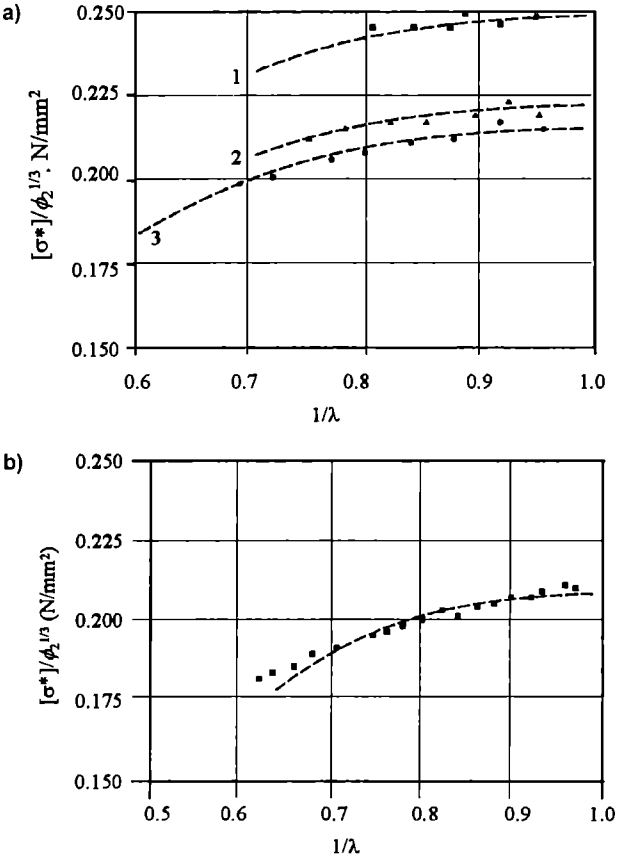

Fig. 10. M-C Mooney-Rivlin curves (----) fitted to experimental data at value of $[\sigma^*]$ at $1/\lambda \sim 0.9$; density of dry network = 974 kg · m^{-3}, T = 293K [27]; a) sample A — dodecane: 1) $\phi_2 = 0.29$, $n_{M\text{-}C} = 271$; 2) $\phi_2 = 0.60$, $n_{M\text{-}C} = 302$; 3) $\phi_2 = 0.80$, $n_{M\text{-}C} = 311$; b) sample A, unswollen: $\phi_2 = 1.00$, $n_{M\text{-}C} = 311$

Correlation with experimental data

The simulated PDMS-network stress-strain data have been compared quantitatively [29] with the experimental results of Erman and Flory [27]. These authors prepared crosslinked PDMS networks, and subjected them to uniaxial extension at various degrees of swelling in dodecane, at approximately 293K.

The experimental values of $[\sigma^*]$ were normalised over $\phi_2^{1/3}$ (where ϕ_2 is the volume fraction of polymer in the swollen network) to give equivalent, dry-network behaviour. The M-C data were transformed to a series of plots of $[\sigma^*]/RT\rho$ versus $1/n$ at constant $1/\lambda$. Simulated values of $[\sigma^*]$ were equated with experimental values of $[\sigma^*]/\phi_2^{1/3}$ at a reciprocal extension of $1/\lambda = 0.9$, to define an effective M-C chain length, $n_{M\text{-}C}$, for each set of experimental results. Note that apart from the most highly swollen network, $n_{M\text{-}C} \approx 310$ bonds to within ±2.5%. The fixing of $n_{M\text{-}C}$ is equivalent to choosing the value of the initial modulus or M_c (*cf.* section 1). Having thus established $(1/n)_{M\text{-}C}$, the simulated Mooney-Rivlin curve was determined from the variation of $[\sigma^*]/RT\rho$ with $1/\lambda$ at that value of $1/n_{M\text{-}C}$. The results are shown in figure 10. It can be seen that the simulated PDMS network behaviour provides satisfactory representations of the experimental data.

CONCLUSIONS

Section 1:

The incidence of unreacted chain ends in a network material can, in principle, is quantified experimentally. Enumerating network defects due to loop structures remains experimentally intractable. A M-C simulation approach, in which the numbers of loop structures formed are weighted according to size and the molecular structures of the reactants, provides a means of generating realistic model network structures, whose topologies are known in full detail. The subsequent correlations between experimentally measured network moduli and extents of loop-forming reaction, calculated via the M-C simulation, show clearly that larger loop structures contribute significantly to the observed loss of elasticity, relative to that of a perfect network.

Current work is focusing on the direct calculation of the entropies of larger loop structures and more exact calculations of P_{ab} for sub-chains in branched structures. From such calculations, moduli can be predicted more accurately, directly from reactant structures and reaction conditions, without the use of semi-empirical values of x and P_{ab} .

Section 2:

The M-C network simulation using chains limited to their natural, conformational full extension (r_{max}) is able to reproduce experimentally-observed deviations from affine, Gaussian network-chain behaviour at moderate uniaxial deformations. The concepts of phantom network and junction-point fluctuations [25—27] are not required. Decreases in the rate of free-energy change with deformation of the network occur naturally as an increasing proportion of network chains becomes fully extended.

The network simulations have recently been extended to interpret stress-optical behaviour [31, 32]. However, further avenues of investigation still need to be explored. As chains reach full extension, the contributions of valence-angle distortion and bond stretching to the network free-energy change need to be investigated. The effects of the co-operative deformation of network chains, such as in loop topologies (see section 1) need to be studied, and the predictions of the model for other modes of deformation need to be examined against experiment.

Overall:

For a complete understanding of the structure and elastomeric properties of polymer networks, the types of investigations in sections 1 and 2 need to be combined. Thus, from investigations of the type described in section 1, the number and types of elastic chain, including loop structures, and their entropy-deformation relationships will be known. The network can then be deformed, as in section 2, and the values of initial modulus as well as stress-strain behaviour predicted.

ACKNOWLEDGEMENT

Support of the EPSRC for grants GR/L/66649 and GR/L/62306 is gratefully acknowledged.

REFERENCES

1. Flory P. J., "Principles of Polymer Chemistry", Cornell University Press, Ithaca 1953.
2. Stepto R. F. T. , chap. 10 in "Comprehensive Polymer Science", 1st Suppl. (Aggarwal S. L. and Russo S., eds.), Pergamon Press, Oxford 1992.
3. Stepto R. F. T., chap. 2 in "Polymer Networks – Principles of Their Formation, Structure and Properties" (Stepto R. F. T., ed.), Blackie Academic & Professional, London 1998.
4. Stepto R. F. T., Cail J. I., Taylor D. J. R., *Macromol. Symp.* (in press, 2000).
5. Mark J. E., Erman B., chap. 7 in "Polymer Networks – Principles of Their Formation, Structure and Properties" (Stepto R. F. T., ed.), Blackie Academic & Professional, London 1998.
6. Graessley W. W., *Adv. Polymer Sci.* 1974, **16**.
7. Doi M., Edwards S. F., *J. Chem. Soc., Faraday Trans. 2* 1978,**74**, 1789, 1802, 1818.
8. Heinrich G., Straube E. and Helmis G., *Adv. Polymer Sci.* 1988, **85**, 34.
9. Kramer O., chap. 17 in "Elastomeric Polymer Networks"(Mark J. E., Erman B., eds.), Prentice Hall, Englewood Cliffs, NJ 1992.
10. Stepto R. F. T., Eichinger B. E., chap. 18 in "Elastomeric Polymer Networks"(Mark J. E., Erman B., eds.), Prentice Hall, Englewood Cliffs, NJ 1992.
11. Gottlieb M., Macosko C. W., Benjamin G. S., Meyers K. O., Merrill E. W., *Macromolecules* 1981, **14**, 1039.
12. Macosko C. W., Saam J. C., *Polymer. Prepr., Div. Polymer Chem., Amer. Chem. Soc.* 1985, **26**, 48.
13. Jacobson H., Stockmayer W. H., *J. Chem. Phys.* 1950, **18**, 1600.
14. Ross-Murphy S. B. Stepto R. F. T., chap.16 in "Large Ring Molecules"(J. A. Semlyen, ed.), Wiley, Chichester 1996.
15. Stanford J. L., Stepto R. F. T., chap. 20 in "Elastomers and Rubber Elasticity, Amer. Chem. Soc. Symp. Series 193"(Mark J. E., Lal J., eds.), American Chemical Society, Washington D.C. 1982.
16. Stepto R. F. T., chap. 10 in "Biological and Synthetic Polymer Networks"(Kramer O., ed.), Elsevier Applied Science, Barking 1988.
17. Taylor D. J. R., Stepto R. F. T., to be published.
18. Dutton S., Stepto R. F. T., Taylor D. J. R., *Angew. Makromol. Chem.* 1996, **240**, 39.
19. Graessley W. W., *Macromolecules* 1975, **8**(2), 186, 865.
20. Lee K.-J., Eichinger B. E., *Polymer, 1990,* **31**, 406, 414.
21. Page E. S., Wilson L. B., "An Introduction to Computational Combinatorics", Cambridge University Press 1979, p. 74 *et seq.*
22. Stepto R. F. T., Taylor D. J. R., in "Cyclic Polymers", 2nd ed.(Semlyen J. A., ed.), Kluwer 1999, in press.
23. Stepto R. F. T., *Polym. Bull. (Berlin)* 1990, **24**, 53.
24. Treloar L. R. G., The Physics of Rubber Elasticity, 3rd ed. Clarendon 1975.
25. Flory P. J., *Proc. Roy. Soc. London, Ser. A* 1976, **351**, 351.
26. Erman B., Mark J. E., *Ann. Rev. Phys. Chem.* 1989, **40**, 351.
27. Erman B., Flory P. J., *Macromolecules* 1983, **16**, 1607.
28. Flory P. J., Crescenzi V., Mark J. E ., *J. Am. Chem. Soc.* 1964, **86**, 146.
29. Stepto R. F. T., Taylor D. J. R., *Macromol. Symp.* 1995, **93**, 261.
30. Stepto R. F. T., Taylor D. J. R., *J. Chem. Soc., Faraday Trans.* 1995, **91**, 2639.
31. Taylor D. J. R., Stepto R. F. T., Jones R. A., Ward I. M., *Macromolecules* 1999, **32**, 1978.
32. Cail J. I., Taylor D. J. R., Stepto R. F. T., Brereton M., Jones R. A., Ries M. E., Ward I. M., *Macromolecules* (in press, 2000).